Journal of ELECTRICAL ENGINEERING, VOL 74(2023), NO2, 132–136

sciendo

COMMUNICATIONS

Study on UV optical field distribution of partial discharge in GIS disconnector based on ray tracing method

Fei Du, Jinpeng Jiang, Shuai Yuan, Jiangang Bi, Yuan Xu[1]

In order to clarify the distribution law of the radiation optical field of the gas insulated switchgear disconnector defect and determine the detection range of partial discharge optical sensor, the optical model of the gas insulated switchgear disconnector based on the uniform geometrical theory of diffraction theory is established based on ray tracing method, and the distribution of the radiation light field is calculated when partial discharge occurs at the key positions such as the basin insulator, shield, and support insulator barrel. Based on the maximum irradiance, average irradiance and attenuation characteristics on the shell interface, the distribution law is further analysed, and based on this, the optimal location of the ultraviolet detector is proposed.

K e y w o r d s: ray tracing, GIS disconnector, partial discharge, UV detection

1 Introduction

Gas insulated switchgears(GIS) are widely used in power grids, its internal conductive rod, insulator and other parts are set in closed shell with high air pressure and high field strength. The condition of the internal parts and the overall operation status of the equipment cannot be directly observed from the outside. In the industry, the detection methods for GIS status are all indirect, mainly including SF6 detection, gas pressure observation, partial discharge(PD) detection, X-ray detection and infrared temperature measurement[1-5]. Gas detection is mainly used to indirectly evaluate the internal insulation status by measuring the change of gas and moisture. PD detection evaluates whether PD occurs in the equipment by detecting the electromagnetic wave and ultrasonic signal. Although these methods can obtain the internal state of GIS to a certain extent, they are all indirect evaluation of the internal state by changing the characteristics of a certain type of signal. Indirect detection methods can only provide a rough judgment and cannot accurately calculate the internal defect position and defect type. The formulation of maintenance strategies for such signals often depends on the technical level and experience of the inspectors, and lacks objective and accurate equipment status information[6-9].

High-energy electrons are produced during gas discharge process, and the energy transfer between electrons and gas molecules will be realized by inelastic collision, resulting in the atoms, molecules and other particles in the discharge area will be excited to the high energy level and be in the excited state. According to quantum theory, the excited state particles will transition to the low energy state with a certain probability, and the excess energy will be radiated in form of photons. PD may occur inside due to internal defects and other reasons. With the increase of voltage, the ultraviolet(UV) region in the corona or PD spectrum increases significantly, and the UV wavelength generated by the discharge is between 280 and 380 nm. In recent years, scholars and institutions have carried out experimental research on the UV spectrum characteristics of GIS internal discharge.

To intuitively describe the internal defects of GIS, UV images are used experimentally by researchers of power grids or research institutions. UV imaging detector is used to conduct experimental research on the internal discharge characteristics of GIS under the condition of linear metal foreign matters attached to the insulator surface. Internal defects of the actual GIS equipment by setting nuts, washers, screws and aluminium wires on the surface of the basin insulator are simulated. However, there are still many problems in UV detection of GIS internal discharge. The internal structures of GIS are complex, which results in great differences in the distribution of UV light emitted by defects at different positions. This difference puts forward more stringent requirements for the installation position of UV sensors. Without considering the installation position and optical transmission characteristics of the sensor, it is difficult to accurately observe the discharge process, which brings great challenges to GIS status assessment.

In this paper, the optical calculation model of GIS disconnector is established by means of ray tracing method. By simulating the UV light signals excited by typical defects such as pot insulator and contact foreign matter, the distribution law of UV light on the shell surface is studied, and the sensor arrangement position which can accurately observe the UV light is proposed.

[1] China Electric Power Research Institute, dufei@epri.sgcc.com.cn

https://doi.org/10.2478/jee-2023-0018, Print (till 2015) ISSN 1335-3632, On-line ISSN 1339-309X

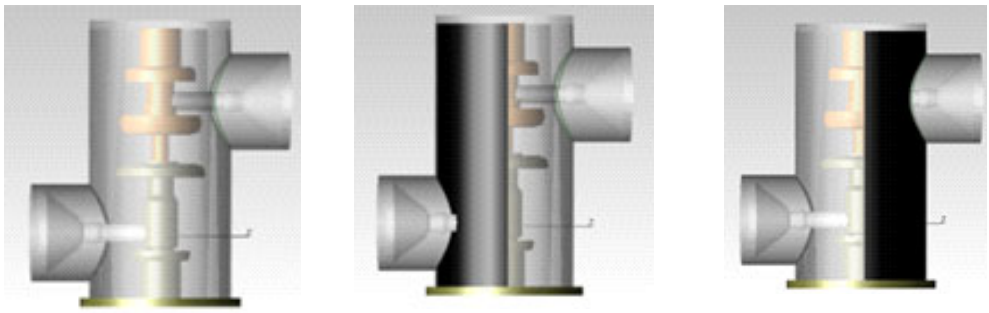

(a) (b) (c)

Fig. 1. Optical calculation model of gis:(a) – optical structure, (b) – left observation surface, (c) – right observation surface

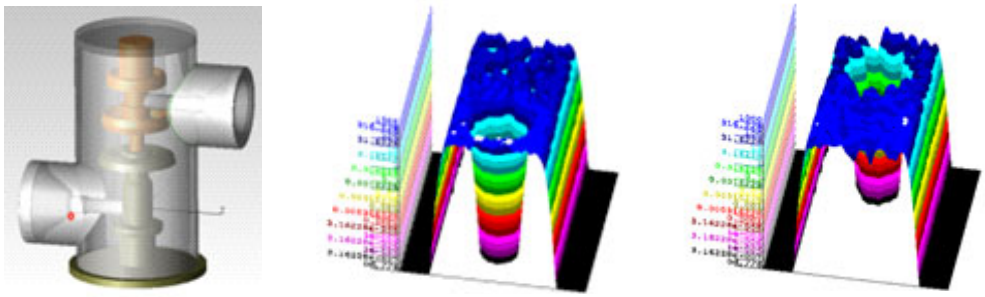

(a) (b) (c)

Fig. 2. Optical field radiated by the defect on the lower basin insulator:(a)UV source, (b) – irradiance on the left shell, (c) – irradiance on the right shell

2 Optical calculation model of GIS disconnector based on ray tracing method

2.1 Ray tracing method and uniform geometrical theory of diffraction

In order to solve the problem of discontinuous field value at the shadow boundary in the geometric optical field, it is necessary to combine the uniform geometrical theory of diffraction(UTD) to study the field value problem in the shadow area. In the consistent geometric diffraction theory, the surrounding rays can exist in both the illumination area and the shadow area. As the field value of the shadow area in geometric optics is zero, all rays with field strength which are not equal to zero in the shadow area are composed of diffracted rays. UTD overcomes the problem of discontinuity of the geometric optical field at the shadow boundary, which further improves the calculation method of the ray field in the illumination area[10]. The basic criteria are:

(1) Diffraction rays follow the generalized Fermat principle. Not only the ray in geometric optics travels along the shortest distance, but also the diffraction ray travels along the shortest diffraction path.

(2) At high frequencies, the reflection, refraction and diffraction phenomena only depend on the geometric and electromagnetic characteristics of the diffraction point and its vicinity.

(3) The outgoing rays after leaving the diffraction point still follow the geometric optics criteria, and the phase difference caused by diffraction is equal to the product of the length of the diffraction path and the number of electromagnetic waves.

Edge diffraction occurs when the ray incident on the edge of the wedge. The incident ray excites numerous diffraction rays to distribute on the Keller cone. The apex

Table 1. The parameters of UV source

Parameters	Value	Unit
Spatial ratio	Uniform luminous flux/position weighting	1
Angular ratio	Uniform luminous flux/angle weighting	1
Wavelength component 0.2 μm	135.5	L_m
Wavelength component 0.38 μm	135.5	L_m

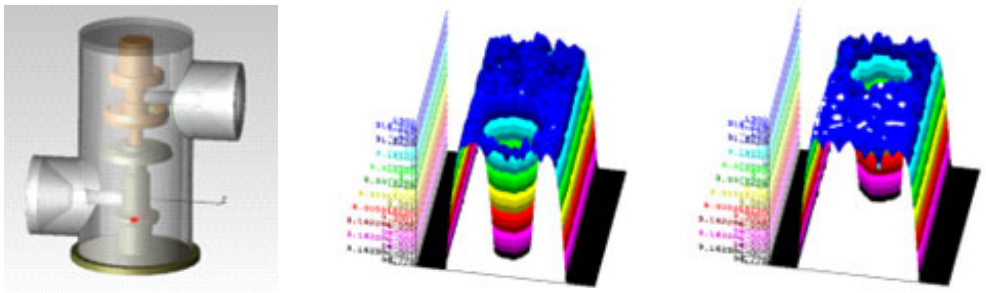

Fig. 3. Optical field radiated by the defect on support insulating cylinder:(a) – uv source,(b) – irradiance on the left shell,(c) – irradiance on the right shell

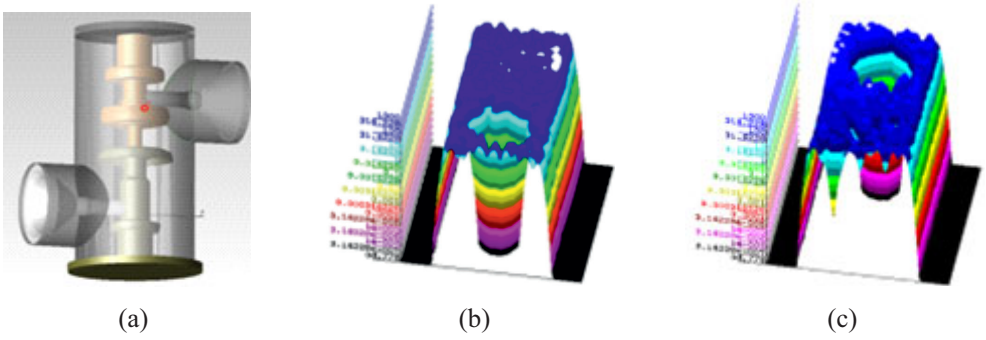

Fig. 4. Optical field radiated by the defect on moving contact shield:(a) – uv source, (b) – irradiance on the left shell, (c) – irradiance on the right shell

of the cone is the intersection point of the incident ray and the edge of the wedge, the axis of the cone is the straight line of the edge, and the semi-apex angle of the cone is the included angle of the incident ray and the edge. Surface diffraction occurs when the ray is incident on a smooth convex surface. Some rays still propagate according to the principle of geometric optics to form refraction, reflection, or direct rays, while the other part propagates along the surface of the surface to form diffraction rays, and radiates countless rays along the tangent direction of the surface.

2.2 Optical calculation model of GIS

Considering that there are many defects such as welding of disconnector cover, foreign matter discharge of shield cover and foreign matter discharge of support insulation cylinder, the UHV GIS disconnector of a certain manufacturer is selected as the research object, and the model is established as Fig. 1.

The UV source is a Gaussian lattice UV source. The starting point of the ray is located on a circular plane distributed according to the Gaussian density. The parameters are shown in Tab. 1

In order to facilitate the actual installation of optical sensor, the detective position is located on the side of GIS, therefore, the shell of GIS is divided into two parts along the axial direction, and the optical distribution of defect UV sources at different positions on the shell is observed respectively.

3 Optical field distribution of typical defect radiation

3.1 Optical field radiated by the defect on the lower basin insulator

The UV source is set on the lower basin insulator, as shown in Fig. 2(a), which simulates the discharge of foreign matters from the insert caused by poor assembly process. The calculation results are shown in Fig. 2.

The result of ray tracing shows that when the UV source is located on the lower basin insulator, the maximum irradiance received by the left observation surface is 615.57 W/m^2, and the average value is 82.91 W/m^2. The maximum value is located at the lower part of the intersection line between the lower branch bus and the isolating switch tank. The maximum irradiance received by the right observation surface is 376.76W/m^2, and the average value is 88.39 W/m^2. The distribution of incident rays shows that the left side is partially dark since the UV source cannot be completely direct, so the average power is smaller. The right side has a large distribution range due to light refraction, reflection and diffraction, and the average power is higher, but the maximum power is re-

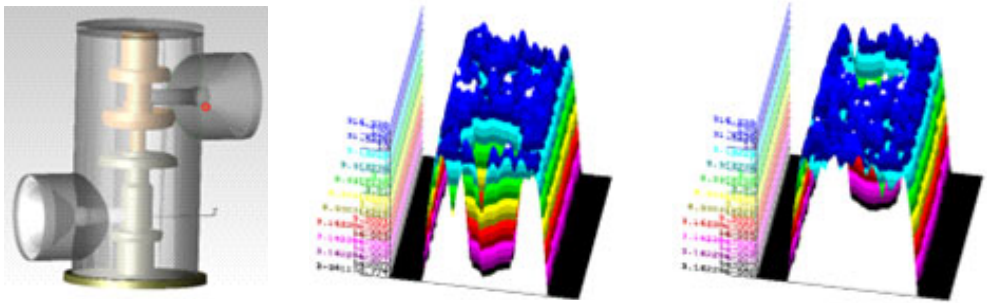

(a) (b) (c)

Fig. 5. Optical field radiated by the defect on higher basin insulator:(a) – uv source, (b) – irradiance on the left shell, (c) – irradiance on the right shell

Table 2. Best observation positions

Component type	Position	Left irradiance	Right irradiance	Best observation position
Lower basin	Ground	314.34	384.34	Lower right
	Conductor	615.57	376.76	Lower right
Lower support	90	615.34	537.02	Lower right
insulating cylinder	0	1021.9	317.19	Lower left/right
bottom	180	401.16	704.94	Lower right
Static	90	772.24	414.82	Lower left/right
contact	0	1304.7	340.98	Middle left, lower right
shield	180	301.02	1493.3	Lower right
Shielding of high	90	1278.8	740.69	Higher left/right
support insulating	0	1230.4	338.05	Higher left/right
cylinder	180	309.08	706.85	Higher left/right
Higher	Conductor	257.43	226.55	Lower right, Higher left/right
basin	Ground	366.86	260.61	Higher left/right

duced by 38.8% due to the attenuation of the propagation process.

3.2 Optical field radiated by the defect on support insulating cylinder

The defect is set at 90 deg of the high pressure equalizing ring, and the radial direction of the defect is perpendicular to the plane of the two branch buses, as shown in Fig. 3(a).

The result of ray tracing shows that the maximum irradiance received by the left observation surface is 384.26 W/m^2, and the average value is 87.922 W/m^2. The maximum value is located at the intersection line of the defect plane and the left observation surface, and part of the light rays are incident to the low branch bus tube. The maximum irradiance received by the right observation surface is 518.23 W/m^2, the average power is 143.96 W/m^2, the maximum value is located at the lower part of the static contact plane, and the distribution range is larger. The distribution of incident rays shows that due to the partial diffraction and reflection of the UV source on the left side to the interior of the lower busbar barrel, the direct light energy is less, and the maximum radiation power is reduced by 25.9% due to the attenuation of the propagation process.

3.3 Optical field radiated by the defect on moving contact shield

The defect is set at 90 deg of the moving contact shield, the radial direction of the defect is perpendicular to the plane of the two branch buses, as shown in Fig. 4(a).

The result of ray tracing shows that the maximum irradiance received by the left observation surface is 662.78 W/m^2, and the average value is 122.11 W/m^2. The maximum value is located near the projection of the plane of the dynamic shield and the left observation surface, which is distributed in bands and close to the defect direction, and part of the UV source diffraction rays intersect with the left observation surface far from the defect direction. The maximum irradiance received by the right observation surface is 458.73 W/m^2, and the average value is 93.06 W/m^2. The maximum position relates to the left observation surface, and the maximum radiation power is reduced by 30.8% due to the attenuation of the propagation process.

3.4 Optical field radiated by the defect on higher basin insulator

Foreign matter is set in the gap of the basin insulator, which may drop and discharge when switch contact moves, and the UV source is set on higher basin insulator, as shown in Fig. 5.

The result of ray tracing shows that the maximum irradiance received by the left observation surface is 257.43 W/m^2, and the average value is 23.80 W/m^2. The maximum value is located on the projection of the moving shield and the shield welded on the left observation surface, which is in a dotted distribution and strip arrangement, and is formed by the UV source scattering and diffraction. The maximum irradiance received by the right observation surface is 226.55 W/m^2, and the average value is 23.94 W/m^2. The maximum value is located at the intersection line and the lower part of the branch bus of the right observation surface, which is formed by the UV source diffraction and the reflected light of the moving contact assembly. The maximum radiation power is reduced by 12.0% due to the attenuation of the propagation process.

4 The best observation positions of UF sensor for different typical defects

In order to calculate the best position observed by the sensor, the optical field radiated by the typical defects of different positions and components is calculated, including the ground potential of the higher and lower basin insulators and the discharge of the embedded foreign matter, the lower support insulator barrel, and the foreign matter defects shielded by the static contact at 0, 90 deg, and 180 deg respectively. The results are shown in Tab. 2.

According to the calculation results, the UV sensor should be installed on the lower right side of the disconnector as far as possible to effectively observe the UV signal radiated by the defect on basin, lower support insulating cylinder bottom and static contact shield.

5 Conclusions

Ray tracing method is used to establish the calculation model of the optical field of GIS disconnector, and the distribution law of the radiation light field of typical defects at different positions of the disconnector is proposed, and the optimal observation position of the sensor is determined accordingly.

(1) UV photons radiated by defects will be refracted, reflected and diffracted due to the influence of insulating parts, conductors and contact shielding during the transmission to the GIS shell.

(2) When the photons can be directly emitted or reflected to the observation surface, the relative attenuation is small, and even the photons can be effectively received through the sensor on the same side of the UV source. While the photons are diffracted and then reflected, the relative attenuation is larger.

(3) UV sensor should be installed on the lower right side of the disconnector as far as possible to effectively observe the UV signal radiated by the defect on basin, lower support insulating cylinder bottom and static contact shield.

The proposed ray tracing method can be applied to other units of GIS, such as circuit breaker and current transformer, and the effective observation positions of different defects are proposed, which provides a new practical basis for GIS condition monitoring.

Acknowledgements

This project is supported by Research on key technologies of multi-spectral optical imaging in GIS based on optical fiber image transmission, the Technical Project of State Grid Corporation of China(5500-202216134A-1-1-ZN).

References

[1] S.-W. Jee and D.-Y. Lim,"Surface discharge mechanism, with a change of gas pressure in N2/O2 mixed gas for insulation design of SF6-free high-voltage power equipment", *IEEE Transactions on Dielectrics and Electrical Insulation*, vol. 28, no. 3, pp. 771-779, 2021.

[2] M. Farajollahi *et al*,"Locating the source of events in power distribution systems using micro-PMU data", *IEEE Transactions on Power Systems*, vol. 33, no. 6, pp. 6343-6354, 2018.

[3] B. Zalba *et al*,"Review on thermal energy storage with phase change: materials, heat transfer analysis and applications", *Applied thermal engineering*, vol. 23, no. 3, pp. 251-283, 2003.

[4] H. A. Kazem and T. C. Miqdam,"Effect of environmental variables on photovoltaic performance-based on experimental studies", *International Journal of Civil, Mechanical and Energy Science*, vol. (IJCMES)2, no. 4, pp. 1-8, 2016.

[5] Y. Zhou *et al*,"Effect of different nanoparticles on tuning electrical properties of polypropylene nanocomposites", *IEEE Transactions on Dielectrics and Electrical Insulation*, vol. 24, no. 3, pp. 1380-1389, 2017.

[6] J. Wang *et al*,"Metal particle contamination in gas-insulated switchgears/gasinsulated transmission lines", *CSEE Journal of Power and Energy Systems*, vol. 7, no. 5, pp. 1011-1025, 2019.

[7] A. Nakajima, *et al*,"GaNbased complementary metaloxidesemiconductor inverter with normally off Pch and Nch MOSFETs fabricated using polarisationinduced holes and electron channels", *IET Power Electronics*, vol. 11, no. 4, pp. 689-694, 2018.

[8] Y. Naka, and I. Hiroyoshi,"Two-dimensional photonic crystal L-shaped bent waveguide and its application to wavelength multi/demultiplexer", *Turkish Journal of Electrical Engineering and Computer Sciences*, vol. 10, no. 2, pp. 245-256, 2002.

[9] J. Yang *et al*,"All-MBE grown InAs/GaAs quantum dot lasers with thin Ge buffer layer on Si substrates", *Journal of Physics D: Applied Physics*, vol. 54, no. 3, pp. 035103, 2020.

[10] J. Arvo and K. David,"Fast ray tracing by ray classification", *ACM Siggraph Computer Graphics*, vol. 21, no. 4, pp. 55-64, 1987.

Received 22 March 2023